Mode I Intralaminar Fracture Toughness in Carbon Fibre Reinforced Polyvinylidene Fluoride (PVDF)

N. Samodajev, M. Hansen, S. Mark

Department of Materials and Production, Aalborg University
Fibigerstraede 16, DK-9220 Aalborg East, Denmark
Email: nsamod16@student.aau.dk, mhha12@student.aau.dk, smark16@student.aau.dk
web page: http://www.mechman.m-tech.aau.dk/

Abstract

Exploration of deep-sea oilfield demands for lighter riser solutions. Material substitution of the heavy pressure steel amour with angle-ply ±80° carbon fibre reinforced Polyvinylidene fluoride (PVDF) tape has been proposed as an alternative material. In this work, a symmetrical layup of 22 layers of carbon fiber reinforced PVDF tape were processed into a test laminate by compression molding and mechanical properties were studied for two fiber orientations (±80° and ±10°) using three-point bending method. An intralaminar fracture toughness test revealed as expected that the fibers aligned almost perpendicular to the crack plane are capable to sustain higher load and therefore producing higher fracture toughness. Samples with fiber oriented ±10° to the crack plane, exhibit crack growth and various bridging mechanisms while in samples with fibre oriented ±80° comprehensive plastic deformation with no detectable crack growth was observed. However, evaluation of plane strain conditions revealed that the dimensions of the samples should be increased for both fibre orientations in order to obtain valid fractures toughness values.

Keywords: Fracture Toughness, Fracture Mode I, Three-point Bending, Carbon Fibre Reinforced Polymer, Polyvinylidene Fluoride (PVDF), Intralaminar Crack Propagation

1 Introduction

Today the oil and gas industry continues to explore and develop deep-sea oilfields which require development of more advanced riser solutions. As the water depth increases and the risers gets longer, there is a demand for designing lighter risers being able to deal with extreme pressure, temperature and corrosive environments [1][2].

In principle, conventional flexible pipes are a multi-layer construction containing a thermoplastic inner liner reinforced with metallic materials [3][8], see Fig.1. Using metallic materials as reinforcement in flexible pipes is a common method in the industry and the material behaviour, fatigue and failure modes are well reported and understood [4].

The advantages of using carbon fibre reinforced polymer materials are well known due to their low density, high specific strength, stiffness and excellent fatigue performance [4][5].
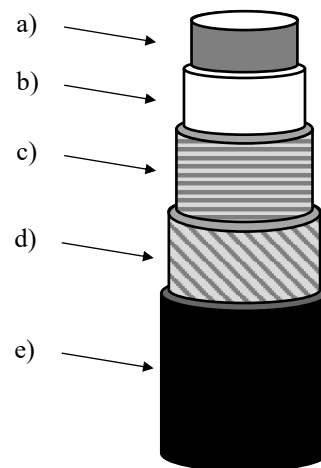
Fig.1. Principle of the conventional flexible pipes. a) Cascass (prevent collapse and provide mechanical protection of the inner liner) b) Thermoplastic inner liner (fluid barrier), c) Steel pressure amour (caring radial loads), d) Steel tensile amour (caring axial loads) and e) Outer sheet (polymer that shield the structural components from the outer environment).

These favourable properties have motivated the industry to take advantage of composite materials as replacement for the heavy metallic materials in the risers [1][6][7].

Recently, research partnerships in the industry has embarked on a development program to qualify a hybrid composite/metal flexible pipe design for deepwater applications. The approach comprises carbon reinforced Polyvinylidene fluoride (PVDF) layer fused to the thermoplastic inner liner and thereby replacing the heavy steel pressure amour [3][4].

PVDF is already a well-known material in the industry and has been used as the thermoplastic inner liner (fluid barrier) due its high chemical resistance, ageing properties and excellent toughness [5].

However, the behaviour and fracture mechanics of composite materials can be complicated since the materials are often heterogeneous in composition and orthotropic or anisotropic in mechanical behaviour. Therefore, various types of damage mechanisms can occur in comparison to damage in other material [9]. In composite materials combination of ductile and brittle failures can be observed. Fracture modes such as delamination (interlaminar fracture), matrix cracking (intralaminar fracture), matrix-fibre debonding, fibre breaking and fibre pull-outs are possible to occur [15].

In fibre reinforced composites the toughness of the material is improved mainly by the effect of bridging, where fibres can act as crack stoppers and postpone the crack growth by absorbing the applied stress [10] [15].

Moreover, strong interface between matrix and fibre is crucial and leads to high fracture toughness [11]. However, the adhesion between carbon fibres and fluoropolymers like PVDF is reported to be poor due to the lack of compatibility between the polymer and carbon fibre [12]. To overcome this problem various chemical treatments and sizing of the fibre are used in order to improve the interfacial bonding. For example; direct- and plasma fluorination of carbon fibres is reported to have positive results on the interfacial adhesion, as the shear strength between carbon fibres and PVDF increases significantly [11][12][13].

Also, the fluorination has shown to increase the critical energy release rate about four and two times for Mode I double cantilever beam and Mode II edge notch flexure test, respectively, by use of unidirectional carbon fibre reinforced PVDF tape [16].

Beside the above-mentioned study, covering delamination, fracture toughness results for carbon reinforced PVDF seems limited and results for intralaminar cracking seems not even reported. In relation to flexible composite pipes, intralaminar crack propagation with matrix cracking, cracks running in the fibre direction and through thickness are assumed to be one of the possible failure modes and that will be the focus of this study. See Fig.2.
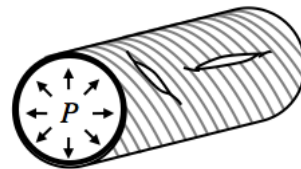
Fig.2. Pressurised pipe section with example of intralaminar crack propagation perpendicular and parallel to the pipe direction.

Intralaminar fracture toughness test is usually carried out by either tension (compact tension specimens) or three-point bending (single end notch end specimens) [15]. Evaluation of intralaminar fracture toughness testing of reinforced polymers, is often referred to ASTM D5045 - Standard Test Methods for Plane-Strain Fracture Toughness and Strain Energy Release Rate of Plastic Materials.

AE Ismal [17] reported a method for performing three-point bending fracture toughness test according to ASTM D5045 on an angle plied woven and unidirectional kenaf fibre reinforced polyester. The fracture mechanisms revealed that the unidirectional fibre configuration perpendicular to the crack were capable to sustain better mechanical deformation and therefore producing higher fracture toughness. Furthermore, the role of fibre orientation revealed different time to failure response.

Intralaminar fracture toughness results have also been reported to be related with interlaminate fracture toughness. According to Pinho [15], interlaminar critical energy release rate can be a good approximation

to describe intralaminar energy release rate for unidirectional laminates. This is based on the assumption that delamination and intralaminar cracking is related to fracture toughness of the matrix and the matrix-fibre interfacial properties [14].

The force-displacement behaviour of angle plied composite laminates exposed to three-point bending load has been reported. Azzam A. and Li W. [9], presented the sensitivity of composites structure with different stacking sequences to a three-point bending load. They found that the material behaviour and failure mode were depended on the stacking sequences and divided the load displacement curves into three regions. First, a linear region explained the elastic deformation of the composite and after the load peak was reached a significant drop due to fibre cracking was observed. Finally, in the third region the specimen continued to support the load with the reinforcement part carrying the load.

However, despite the proposed advantages of introducing carbon fibre reinforced PVDF in flexibles pipes it requires knowledge of its fracture mechanical behaviour due to the extreme operations conditions and potential environmental effects related to failure. As reported, current research seems limited to only unidirectional cases and interlaminar fracture mode (delamination). In this study, the mechanical properties and intralaminar fracture toughness of angle-ply carbon fibre reinforced PVDF tape will be investigated by use of three-point bending test method. Furthermore, a flexural test will be conducted in order to measure the yield strength of the composite to evaluate whether plane strain conditions are obtained.

2 Method

2.1 Material

The investigated material is unidirectional carbon fibre reinforced Polyvinylidene fluoride (PVDF) prepreg with a thickness of 0,25 *mm* and a fibre volume fraction of 45 *%*. The melting temperature were analysed by DSC and found to be 169 *°C*.
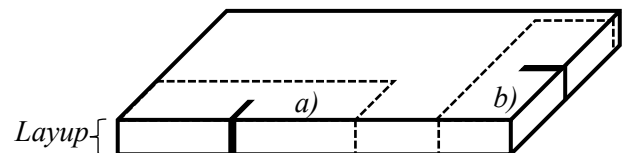
2.2 Samples

Test samples of ±80° carbon fibre reinforced PVDF composite laminates were prepared by cutting the as-

produced composite prepreg into 65 x 258 mm tapes. A total of 22 layers of tape were stacked symmetrically (see Fig.3.) between two steel plates with an area of 120 x 300 mm and a thickness of 10 mm. On each side of the composite parchment papers were used for releasing purpose. Furthermore, 6 bolts tightened by hand, were used to provide pressure during heating. The mould containing the stacked composite tapes was placed in a furnace (Nabertherm) at 235 °C for 60 minutes. The mould was then cooled to ambient temperature before the material was removed.
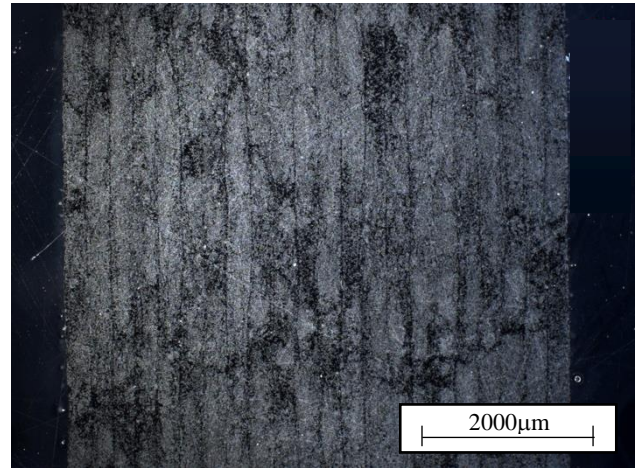

Fig.3. Cross-section of produced composite laminate. 22 layers with a fibre orientation of ±80°. 2,5x magnification.

A total of 16 test samples were prepared, eight test samples with the fibre orientation of ±80° and eight test samples with fibre orientation of ±10°, see Fig. 4. Five test samples from each fibre orientation were made for single edge notch bend (SENB) samples, to determine the fracture toughness, K_{Ic}. Three test samples from each fibre orientation were made for flexural test to determine the yield strength, σ_y and flexural modules, E_f.

Fig.4. Orientation of SENB samples. a) samples with fibre direction of ±10° to the crack plane b) samples with fibre direction of ±80° to the crack plane.

The geometry and dimensions of the SENB samples were based on requirements of ASTM D5045 (Standard Test Methods for Plane-Strain Fracture Toughness and Strain Energy Release Rate of Plastic Materials). The dimensions of the test samples for flexural test were chosen to be the same as for the SENB samples, without notch and pre-crack. The test samples were cut to the required dimensions using a circular saw (Struers Discotom 6) with a cutting speed of 0,5 mm/s and simultaneous cooled to avoid heat effects. See Table 1 for nominal dimensions of test samples.
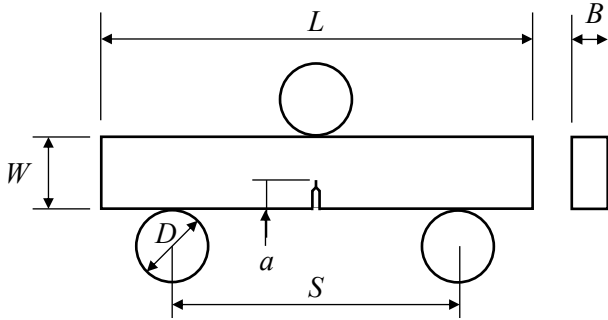
Fig.5. Geometry of the single edge notched bending sample (SENB) and test fixture.

Table 1. Geometric relations from ASTM D5045 and nominal sample dimensions for test.

Dimension	Geometric relations	Size [mm]
B	W / 2	5
W	2 x B	10
L	2 x (2.2 x W)	44
a	0,45-0,55 x W	5
S	4 x W	40
D[1]	W/2 to W	10

[1] *The support rollers deviate from ASTM 5045 and are measured to 15 mm.*

2.3 Notching and pre-cracking

To obtain reproducible fracture toughness results it is important to create uniform notches and pre-cracks. Moreover, it is important to minimize the residual stress around the crack [18] [19].

In this work, initially the composite sample is placed between two wood plates and fixed in a vice to avoid burrs and fibre pull-outs. Then, a notch of 4 *mm* is machined using a hacksaw.

In order to generate a sharp natural crack, a special setup was made. A fresh snap-blade with a thickness of 0,5 *mm* was fixed in an electromechanical testing

machine (Zwick Z100). The vice including composite sample with notch were aligned underneath the snap-blade. Finally, the snap blade was forced 5 *mm* into the composite sample given a pre-crack length of 1 *mm*, see Fig.6 and Fig. 7.

After fabricating the SENB samples, the initial crack length, *a,* was measured on each side using a microscope (Zeiss Imager M2).
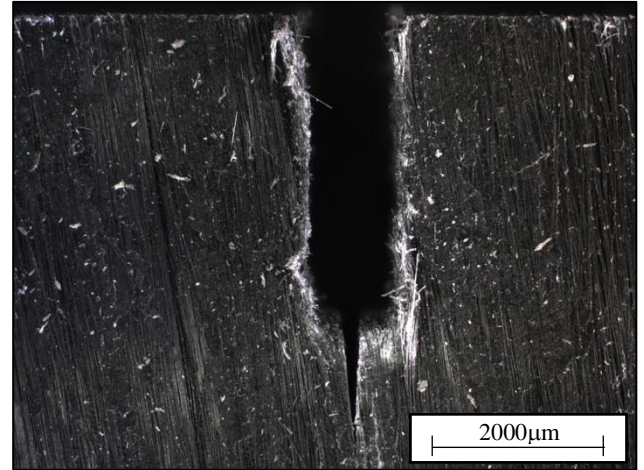
Fig.6. Example of notch and pre-crack. 2,5x magnification.

Fig.7. Example of SENB sample ready for test.

2.4 Flexural tests

Each sample was loaded in a three-point bending fixture equipped with 100 *kN* load cell (Zwick Z100). The crosshead speed was set to 2 *mm/min* and the samples were tested until failure at room temperature. Throughout the experiment the loading force versus displacement was logged using a computer and the side of the samples was recorded using a digital camera (Point Grey – Edmund Optics 75mm).

The yield strength of the samples was calculated using the following equation:

$$\sigma_y = \frac{3PS}{2bW^2} \qquad (1)$$

4

where S is the length between the support, b is the width of the sample, W is height of the sample and P is the load at which yielding is observed (when plastic deformation occurs and where the load displacement curve deviates from linearity).

Furthermore, the flexural modulus, E_f, was calculated by:

$$E_f = \frac{S^3 m}{4bW^3} \quad (2)$$

where m is the slope of the linear part of the force-displacement curve. Also, the fracture zone was investigated by use of stereomicroscope (Lecia MZ6).

2.5 Mode I intralaminar fracture toughness test

The mode I intralaminar fracture toughness was determined by the three-point bending method with SENB samples and fixture shown in Fig.7 and Fig.5. The test was conducted by use of same setup and test parameters as for the flexural test, however the SENB samples were only tested until 5 mm of displacement.

The fracture toughness (critical stress intensity factor) was determined by:

$$K_{Ic} = \sigma F_I(\alpha)\sqrt{a} \quad (3)^*$$

*) Based on the Stress Intensity Factors Handbook Volume 1 JSMS, corrected with a factor of $\sqrt{\pi}$ in order to obtain a valid boundary condition (1,12 for a ≪ W).

where a is the initial crack length, $F_I(\alpha)$ is the shape factor and σ is the nominal stress. The nominal stress was calculated from Eq. 1 using the load P at a compliance of 5% greater than the initial on the force-displacement curve, according to ASTM D5045. The shape factor, $F_I(\alpha)$ over the range ($0 < \alpha < 1$) was determined by:

$$F_I(\alpha) = \frac{1{,}99 - \alpha(1-\alpha)(2{,}15 - 3{,}93\alpha + 2{,}7\alpha^2)}{(1+2\alpha)(1-\alpha)^{3/2}} \quad (4)$$

The resulting K_{Ic} was checked for plane strain conditions. For the plane strain conditions, all characteristic lengths of the sample (B, a, W-a) should comply with

the following:

$$B, a, (W-a) > L_{Critical} = 2{,}5\left(\frac{K_{Ic}}{\sigma_y}\right)^2 \quad (5)$$

where the yield strength, σ_y, is determined by the flexural test.

3 Results and discussion

3.1 Flexural test results

A flexural test was used to determine the yield strength and flexural modulus for the carbon fibre reinforced PVDF composite. All measurements were repeated with three identical samples for each fibre orientation respectively ±80° and ±10°, see Fig.8 and Fig.9.
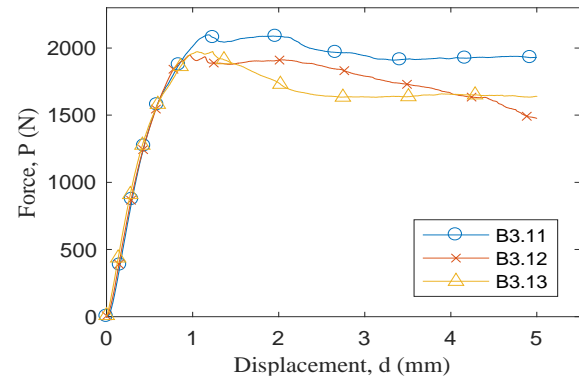

Fig.8. Force-displacement curve for the samples with ±80° fibre orientation.
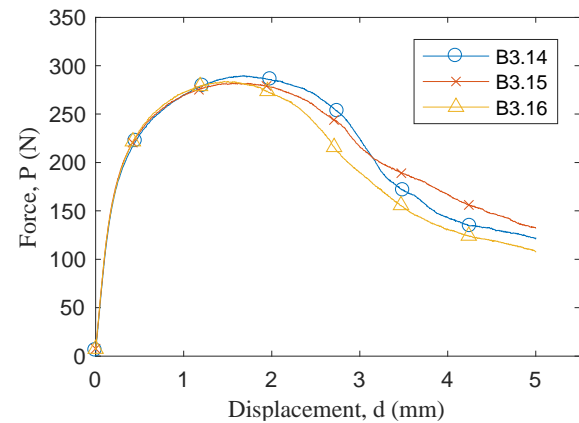
Fig.9. Force-displacement curve for the samples with ±10° fibre orientation.

5

In Fig. 8, the fibres are almost perpendicular to the load, with a peak load varying from 1945 *N* (Sample No. B3.12) to 2097 *N* (Sample No. B3.11). Even though the drop of the peak load in the force-displacement curve is noticeable, the reinforcement continued to carry the load. Furthermore, during this stage major plastic deformation is observed at the top of the samples, as well failures such as delamination and fracture of the fibres occurred, see Fig.10.
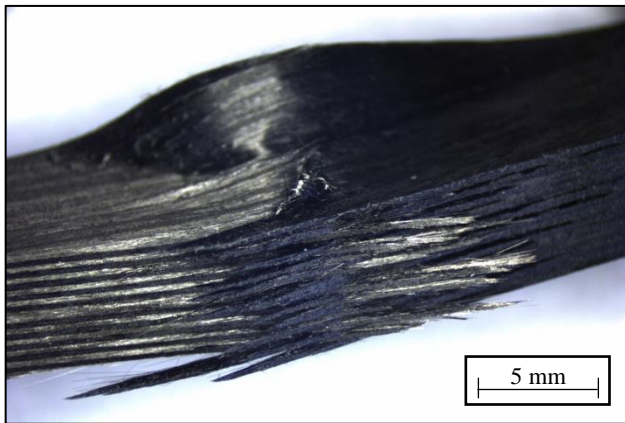
Fig.10. Observed fracture in microscope at the bottom and side of sample B3.11 (fibre oriented ±80°) after 5 *mm* of displacement.

In Fig.9, the fibres are almost parallel to the load, with a peak load varying from 282 *N* (Sample No. B3.15) and 297 *N* (Sample No. B3.14). As for the samples with a fibre orientation of ±80° a drop in peak load was observed, however the drop for the samples with fibre orientation of ±10° was more abrupt and significant for the same displacement. The observed difference in strength is due to the difference in fibre orientation, since the fibres are the load caring agent and stronger and stiffer compared to the matrix. For the samples with a fibre orientation of ±10° no fibre breaking was introduced, instead bridging mechanisms such as fibre pull-outs and miss-aligned fibres were observed, see Fig.11.
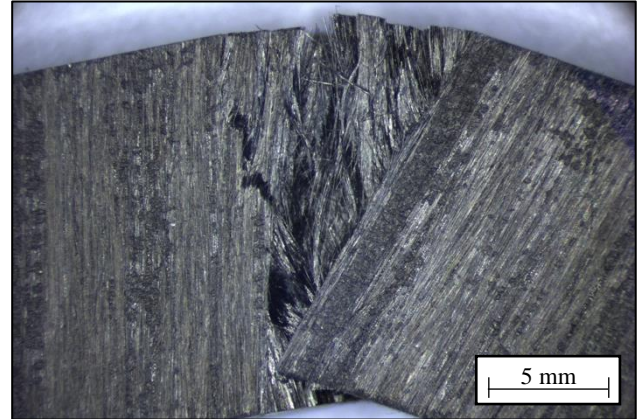
Fig.11. Observed fracture in microscope at the side of sample B3.11 (fibre oriented ±10°) after 5 *mm* of displacement.

Since the change from elastic to plastic behaviour of the samples wasn't clearly defined by a certain yield point on the force-displacement curve, an offset of 0,2% permanent deformation was used to describe the yield strength. The samples with a fibre orientation of ±80° and ±10° exhibit a yield strength of respectively 108,8± 11,0 *MPa* and 13,2± 0,5 *MPa*, see Table 2.

The flexural modules for samples with a fibre orientation of ±80° and ±10° were respectively calculated to be 28,62±5,19 *GPa* and 4,06±0,10 *GPa*, see Table 2. Extensive plastic deformation and ductile behaviour were noticeable on both fibre orientations, however the samples with a fibre orientation of ±80° retained higher strength and stiffness.

**Table 2.** Results of flexural test obtained in three-point bending.

Sample No.	Fibre orientation	W [mm]	B [mm]	P [N]	σ_y [MPa]	E_f [GPa]
B3.11		11,2	5,7	1113	93,2	22,61
B3.12	± 80°	9,7	5,7	1052	118,4	35,28
B3.13		10,4	5,7	1183	101,5	27,98
Mean ±st.dev.		10,4 ± 0,76	5,7 ± 0,01	1116±53,5	108,8± 11,0	28,62±5,19
B3.14		10,3	5,8	144	13,9	4,01
B3.15	± 10°	10,6	5,8	138	12,7	4,20
B3.16		10,6	5,8	139	12,8	3,98
Mean ±st.dev.		10,5 ± 0,14	5,8 ± 0,01	140±2,6	13,2± 0,5	4,06±0,10

3.1 Mode I intralaminar fracture toughness results

In order to evaluate whether the samples deform linear elastic during crack growth a number of unloading was made to see if the samples go back to its original position. Potential non-linear elastic behaviour can be described by the three possible cases; residual stresses, plastic energy dissipated during fracture or crack plane interference effects that will prevent the unloading e.g. partially removed fibres which cannot slide back to its original position [20].
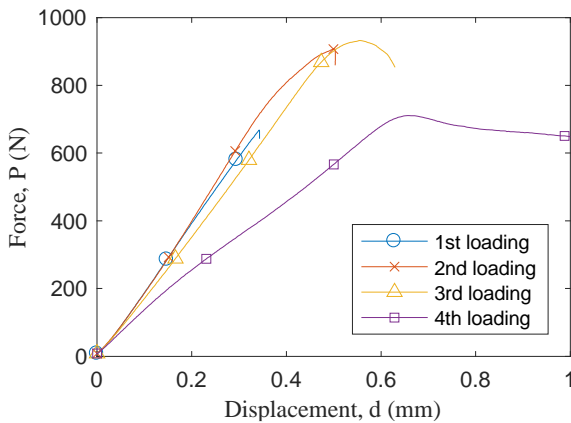
Fig.12. Loading-unloading of sample B3.5 with a fibre orientation ±80° to crack plane. Plastic energy was dissipated during the fourth loading.
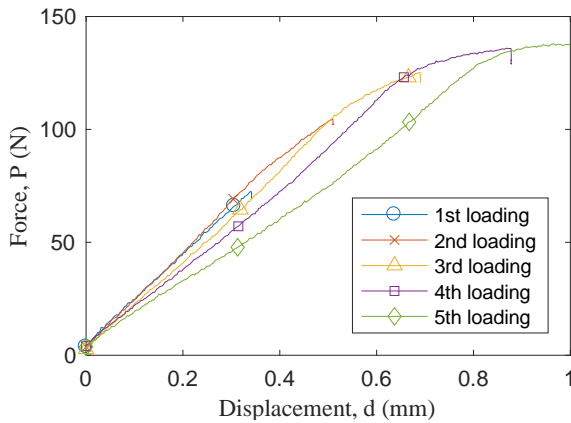

Fig.13. Loading-unloading of sample B3.10 with a fibre orientation of ±10° to crack plane. Crack plane interference effects observed after fourth loading.

For the sample with a fibre orientation of ±80° to the crack plane four loadings were made. The first three loadings showed almost similar characteristics i.e. same slope of the force-displacement curves, see Fig.12. Also, the pictures recorded during loading

shows that the sample goes back to the initial position. For the third loading the peak load of the sample was reached, which resulted in permanent plastic deformation and a change in slope of the force-displacement behaviour for the subsequent loading. However, no crack growth was visually observed during this process.

For the sample with a fibre orientation of ±10° to the crack plane same initial behaviour (1st to 4th loading) was observed as for the ±80° samples, see Fig.13. Nevertheless, the ±10° sample revealed visual crack growth during the linear elastic loading. Moreover, at the fourth loading, the peak load was reached and the sample started to behave non-linear. After unloading, the sample did not return to its original position due to crack plane interference effects. For the subsequent loading, a change in slope of the force-displacement was observed.
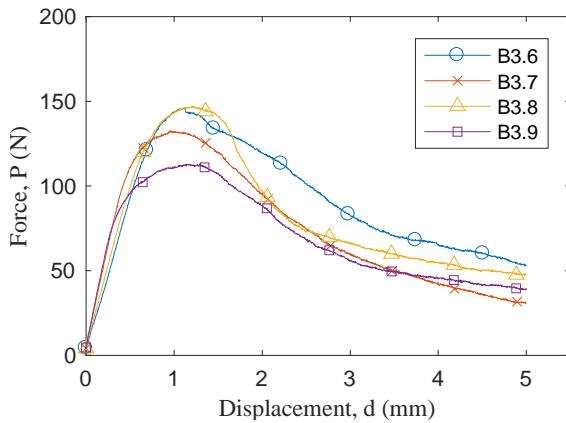
In Fig.14 the force-displacement response of four samples with a fibre orientation of ±80° to the crack is presented. Each four samples showed almost identical response with initially linear elastic deformation until the peak load was reached. The peak load varied from 897 N (Sample No. B3.4) to 1068 N (Sample No. B3.2). During the linear elastic deformation of the samples, the cracks started to open due to tension in the bottom, but no visual crack growth was observed, see Table 3 (Sample No. B3.2).
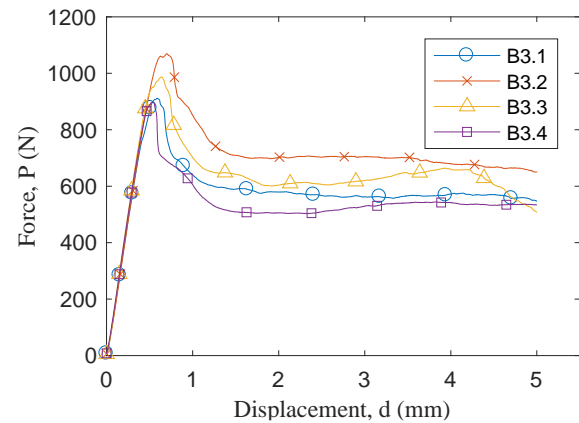
Fig.14. Force-displacement curves of samples with a fibre orientation ±80° to crack plane.

When the peak load was reached, the samples showed local comprehensive plastic deformation under the applied load, which lead to a drop in the force-dis-

placement curve. Furthermore, at the top of the sample, in the area in compression, the laminates started to buckle which resulted in delamination under the applied load, see Fig.16. Due to these observations, the failure mode of the ±80° samples are expected to be governed by plastical deformation rather than crack growth.

Fig.16. Top view of samples with a fibre orientation ±80° to crack plane after testing.

Fig.15. Force-displacement curves of samples with a fibre orientation ±10° to crack plane.

In Fig.15. the force-displacement response of four samples with fibre orientation of ±10° to the crack is presented. As it was expected, by comparing Fig.14. and Fig.15. the strength of the samples with a fibre orientation of ±10° was much lower than for the samples with ±80°. Moreover, for the ±10°, all four samples showed almost identical response with initially linear elastic deformation until the peak load was reached. The peak load varied from 112 N (Sample No. B3.9) to 146 N (Sample No. B3.8). During the linear elastic deformation of the samples, visual detectable crack growth was observed.

From the literature, it is known that fracture of the fibre reinforced composites is highly influenced by the orientation of the fibres [21]. Furthermore, for the samples with fibres oriented ±10° to the crack plane, the fibres are almost parallel to the fracture, which resulted in crack propagation through the matrix at, or close to the fibre matrix interphase with no fibre fracture observed, see Table. 4. The observed crack propagation can be divided into two groups; One where the crack started to open during the linear elastic loading and after a certain load the crack tip becomes less distinct and a crack bridging zone with a combination of unbroken fibre pull-outs and misaligned fibres parallel to crack propagation direction, were observed. A second group of samples with undefined crack tip and subsequent growth during the entire loading. See Table 4 (respectively Sample No. B3.8 and B3.7).

Table 3. Results of fracture toughness test obtained in three-point bending.

Sample No.	Fibre orientation	W [mm]	B [mm]	a [mm]	P [N]	K_{Ic} [MPa·m^0,5]	L_{crit} [mm]
B3.1		9,7	5,7	4,65	761	>13,9	40,5
B3.2		9,8	5,6	4,70	918	>16,7	58,9
B3.3	± 80°	9,9	5,7	4,53	862	>14,3	43,5
B3.4		9,9	5,7	4,72	788	>13,9	41,0
B3.5		10,0	5,7	4,84	919	>16,3	56,1
Mean ± st.dev.		9,9 ± 0,10	5,7 ± 0,04	4,77 ± 0,11	850±65	>15,0±1,2	48,0±7,9
B3.6		10,6	5,8	4,90	128	1,9	53,4
B3.7		10,4	5,8	4,72	102	1.5	33,5
B3.8	± 10°	10,4	5,8	4,77	108	1,6	39,2
B3.9		10,4	5,8	4,73	78	1,2	19,9
B3.10		10,6	5,8	4,65	122	1,7	40,7
Mean ± st.dev.		10,5 ± 0,10	5,8 ± 0,02	4,80 ± 0,09	108±17	1,6±0,2	37,4±10,9

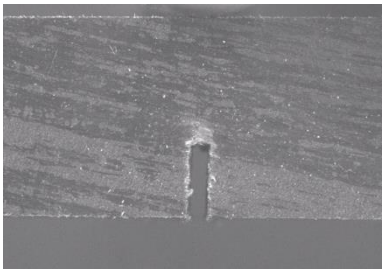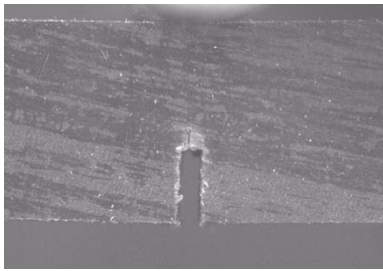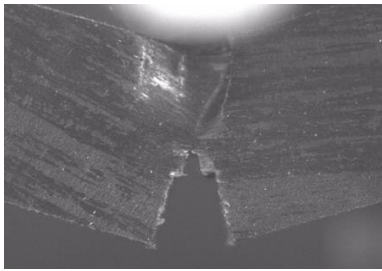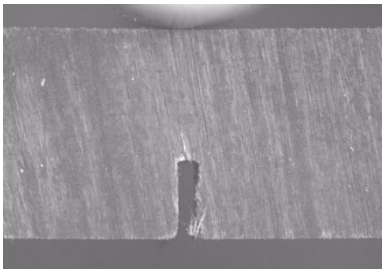**Table 4.** Crack propagation of chosen SENB samples at different load levels.
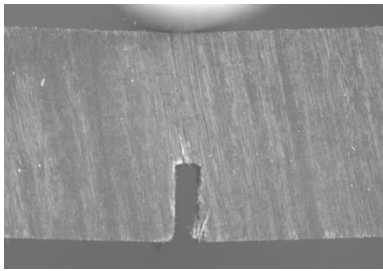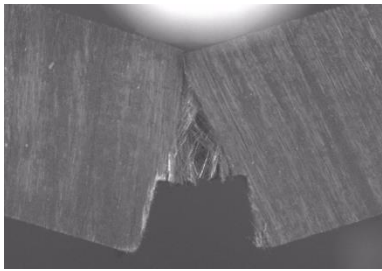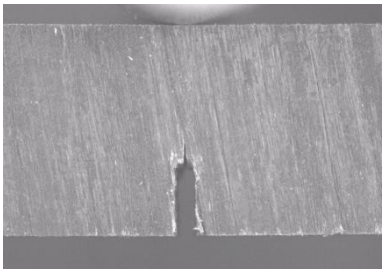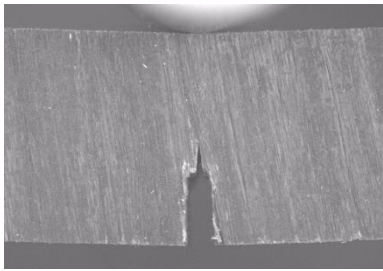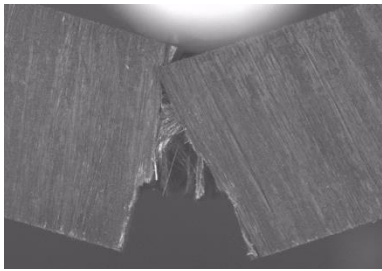
Sample No.	Position on the force-displacement curve		
	Intial stage	K_{Ic}	5 *mm* of displacement
B3.2: (±80°) No crack growth			
B3.7: (±10°) Un-defined crack tip			
B3.8: (±10°) Defined crack tip			

Table 3 shows the results of the 10 fracture toughness samples investigated in the present work. From the table it can be observed, that none of the samples complied with the geometrical constraints for domination of plane strain during crack propagation (Eq. (5)). Furthermore, trials of calculating the R-curve i.e. the K_{Ic} dependency of crack length show non-steady state behaviour which supports the need for increased sample size.

From the fracture toughness results it can be assumed that the ±80° samples as the minimum have an average fracture toughness of 15,0±1,2 $MPa\cdot m^{0,5}$. The calculated average fracture toughness results for the ±10° showed 1,60±0,2 $MPa\cdot m^{0,5}$.

Deviations in fracture toughness values within same fibre orientation group might be explained by differences like; notch and pre-crack geometry, sample tolerances, variations in donated pre-preg tape, errors in laminate from moulding process and alignment of sample in test fixture.

4 Conclusion

In this work, the fracture toughness of carbon fibre reinforced PVDF was investigated. A symmetrical layup of 22 layers with a fibre orientation of ±80° and ±10° to the crack plane were analysed by three-point bending. The two investigated fibre orientations resulted in two different fracture characteristics.

The samples with a fibre orientation ±10° exhibits visual detectable crack growth. During the linear elastic loading the crack started to open and after a certain load the crack tip becomes less distinct and a crack bridging zone with a combination of unbroken fibre pull-outs and misaligned fibres parallel to crack prop-

agation direction, were observed. The calculated average fracture toughness were found to be 1,6 $MPa \cdot m^{0,5}$.

The samples with a fibre orientation of ±80° exhibit comprehensive plastic deformations and a very ductile behaviour with no crack growth. Due to these observations, the failure mode of the ±80° samples are expected to be governed by plastic deformation rather than crack growth. From the fracture toughness results, it can be assumed that the ±80° samples as the minimum have an average value of 15,0 $MPa \cdot m^{0,5}$.

Nevertheless, the obtained fracture toughness values are not valid since no plane strain condition were achieved. In order to obtain valid fracture toughness values the sample size must be increased for both fibre orientations. However, the results still give good indications of the material behaviour and expected failure mode

Acknowledgement

References

[1] M. Thomas "Rising to the challenge". *E&P*, 2013.

[2] S. Whitfield "Current Developments in the world of risers". *Society of Petroleum Engineers*, 2015.

[3] T. A. Anderson, M. E. Vermilyea, V. Jha, N. Dodds, D. Finch and J. R. Latto "Qualification of flexible fiber-reinforced pipe for 10,000-foot water depths*". Offshore Technology Conference*, Houston, 2013.

[4] V. Jha, N. Dodds, D. Finch and J. Latto, G. Karabelas, T. A. Anderson, P. Baehmann and M. E. Vermilyea, "Flexible Fiber-reinforced Pipe for 10,000-foot Water Depths: Performance Assessments and Future Challenges*". Offshore Technology Conference*, Houston, 2014.

[5] S.-R. Shamsuddin, J. Hodgkinson, L. Asp, R. Långstöm and A. Bismarck, "Carbon Fibre Reinforced PVDF Composites"*, ECCM15 – 15th European Conference on composite materials,* Venice, 2012.

[6] "Catenary composite risers", *CompositesWorld*.

[7] J. Backman, "Deepwater risers steel catenary, flexible risers battle for technical supremacy". *Offshore*, 1996.

[8] National Oilwell Varco, http://www.nov.com/ Segments/Completion_and_Production_Solutions/ Subsea_Production_Systems/Flexible_Pipe_Systems/ Designing_Flexible_Pipes/Materials_and_Profiles/ Materials_and_Profiles.aspx.

[9] Azzam A, Li W ''An experimental investigation on the three-point bending behaviour of composite materials'' *IOP*, 2014.

[10] School of Material Science and Engineering, Sydney, http://www.materials.unsw.edu.au/tutorials/online-tutorials/3-toughening.

[11] K. K. Chee Ho, A. F. Lee '' Fluorination of carbon fibres in atmospheric plasma''. Elsevier, 2007.

[12] S. R. Shamsuddin '' Carbon Fibre Reinforced Poly(vinylidene Fluoride). Department of Chemical Engineering, Imperial College London, London, UK,2012.

[13] S. Shamsuddin, Kingsley K.C Ho. '' *Synergy of matrix and fibre modification on adhesion between carbon fibres and poly''*. Elsevier, 2011.

[14] M. W. Czabaj, J. G. Ratcliffe ''Comparison of Intralaminar and Interlaminar Mode-l Fracture Toughness of Unidirectional IM7/8552 Graphite/Epoxy Composite.

[15] M. S. Sham Prasad, C. S. Venkatesha, T. Jayaraju ''Experimental Methods of Determining Fracture Toughness of Fiber Reinforced Polymer Composites under Various Loading Conditions''. Journal of Minerals & Materials Characterisation & Engineering. Vol. 10, No 13, pp 1263-1275, 2011, USA.

[16] K. K. C. Ho, S. Shamsuddin, M. Laffan, A. Bismarck, Uniderictional carbon fibre reinforced poly (vinilidene fluoride): Impact of atmospheric plasma on composite performance" *Elsevier*, 2011.

[17] AE Ismal, SH Masran, S. Jamian, KA Kamarudin, MK Mohd Nor, NH Muhd Norm, AL, Mohd Tobi, MK, Awang, "Fracture toughness of woven kenaf fibre reinforced composites", *International Engineering Research and Innovation Symposium*, 2016.

[18] N. Kuppusamy, R. A. Tomlinson "Repeatable precracking preparation for fracture toughness testing"*,* Elsevier, 2016.

[19] B. C. Kim, S. W. Park, D. G. Lee, "*Fracture toughness of nano-particle reinforced expoxy composite*" Elsevier, 2008.

[20] N. Matsumoto and J. A. Nairn, "Fracture Toughness of MDF and other Materials with Fibre Bridging", *Proc. of 22end Ann. Tech. Conf. of the Amer. Soc. of Composites,* 2007.

[21] D. Hull, ''Fractography: Observing, Measuring and Interpreting Fracture Surface Topography", Cambridge University Press, pp 312-327, 1999, UK